BioNanoScience (2023) 13:1250–1261
https://doi.org/10.1007/s12668-023-01156-4

Enhanced Bactericidal Efficacy of ZnO Nanoparticles in Conjugation with Different Antibiotics

D. V. Surya Prakash[1] · Kuldeep Roy[2] · Sandeep Sirohi[3]

Accepted: 25 June 2023 / Published online: 10 July 2023

Abstract
In this study, the antibacterial activity of ZnO nanoparticles (NPs) with several antibiotics viz. ciprofloxacin, ampicillin, and gentamicin was studied. The ZnO NPs were functionalized with an amine group using (3−aminopropyl) triethoxysilane (APTES), followed by conjugation with antibiotics using EDC and NHS compounds. Nanoparticles were characterized by transmission electron microscopy (TEM), scanning electron microscopy (SEM), X-ray diffraction (XRD), and UV–visible spectroscopy analysis. SEM and TEM analysis confirmed the hexagonal-shaped ZnO NPs with a 20–24-nm range. Similarly, the crystallinity of ZnO NPs was observed with an XRD analysis. The antimicrobial activity of bare ZnO NPs and antibiotics and the synergistic impact of ZnO NPs + antibiotics were evaluated against six bacterial species. *Klebsiella spp*. was extremely sensitive to all three antibiotics, and *Streptococcus spp.* was most responsive to ampicillin. The mechanisms of the antimicrobial behavior of functionalized ZnO NPs were discussed. *E. coli* was selected for CFU measurement to identify colony formation in different dilutions of ZnO NPs. ToxTrak™ test was used to assess the toxicity of chemically synthesized ZnO NPs; 75.86% and 66.76% inhibition were obtained for gram-positive (*B. subtilis*) and gram-negative (*E. coli*) bacterial strains, respectively.

Keywords ZnO NPs · Amine-functionalization · Antibiotics · ToxTrak™ test · *E. coli*

1 Introduction

Nanotechnology is an area of science concerned with generating and utilizing a nano range of materials. It is widely employed in several biomedical applications like drug delivery, diagnostic techniques, antimicrobial wraps, sunscreens, and disinfectants as a catalyst for increasing efficiency. Nanobiotechnology is a branch of nanotechnology that develops and applies technologies to study biological activities. In the current scenario, nanoparticles (NPs) have evolved as a new antimicrobial effect to destroy microorganisms. Due to its unique inhibition properties, researchers have shown huge interest in synthesizing controlled, shaped nanoparticles and their combinations with antibiotics/resistance stains. Some metals/oxides, such as CaO, MgO, ZnO, ZrO, CuO, AgO, and TiO_2, have been demonstrated to exhibit significant antibacterial properties [1–3]. The majority of recent studies in the field of antimicrobial characteristics of biocomposites have focused on ZnO NPs, and several of them have produced promising results [1, 3–9]. The recent development in porous and nanometric materials prepared by conventional methods has opened new vistas in the field of zinc oxide nanoparticles. Synthesis and characterization of nano-scale substances have been an important subject of discussion in applied sciences. The synthesis of metal oxides has made it possible to utilize the properties of nanoparticles in biomedical applications.

ZnO NPs, one of the most significant metal oxide NPs, are widely employed in several fields of applied sciences because of their physical and chemical properties. ZnO NPs have superior antimicrobial, optical, high catalytic activity,

D. V. Surya Prakash and Kuldeep Roy contributed equally to this work.

✉ Sandeep Sirohi
sirohi.iitkgp@gmail.com

[1] Department of Biotechnology, Meerut Institute of Engineering and Technology, Meerut, Uttar Pradesh 250005, India

[2] School of Chemical Engineering, Vellore Institute of Technology, Vellore, Tamilnadu 632014, India

[3] Department of Botany, Hariom Saraswati PG College, Haridwar, Uttarakhand 247667, India

anti-inflammatory, wound healing, antifungal, and excellent UV-blocking properties. ZnO NPs are used as effective materials for antimicrobial agents in surface coating systems, plastics, medical fields, cosmetics, and textile industries [8]. However, when ZnO NPs are reduced to nano-sized, it shows anomalous characteristics compared to their conventional materials. These unique features of ZnO NPs have increased surface area, which allows nanoparticles to interact with bacteria more effectively. It has resulted in a smaller amount of ZnO NPs for the improvement of fungistatic and biostatic behavior. The antimicrobial potential of ZnO NPs acts as an agent in the range of micro and nano-scales for diagnostics and clinical activities. ZnO NPs exhibit bactericidal or bacteriostatic activities against gram-positive and gram-negative bacteria. Furthermore, these nanoparticles showed antibacterial activity against spores, which are known for their resistance to pressure and temperature. Yamamoto (2001) [10] studied the influence of particle size on the antibacterial activity of zinc oxide. The antibacterial activity of ZnO NPs increased with decreasing particle size and increasing powder concentration. Supplementary Table S1 shows the different functionalization of ZnO NPs.

The successful use of multifunctional nanoparticles would be of utmost importance for developing theranostic nanomedicines. However, much research is needed in the clinical translation of nanoparticle probes and solving the underlying problems such as biocompatibility, *in vivo* and *in vitro* targeting efficiency and toxicity. The toxicity of ZnO NPs was estimated in microbial gut microflora by applying the ToxTrak™ test. The earlier investigation found that resazurin dye (7-Hydroxy-3H-phenoxazin-3-one 10-oxide) is a blue color dye and non-fluorescent in nature. It is utilized to measure cell viability in assays due to its oxidation reduction indicator property for microbes and mammalian cells. Earlier researchers utilized resazurin dye for quantitatively estimating bacterial content in milk and indicator for mammalian cell cultures viability [11, 12]. The present research describes the synthesis of ZnO NPs and their functionalization of ZnO NPs. Structural properties of ZnO NPs and functionalized ZnO were analyzed. The antibacterial activities of bare ZnO NPs, antibiotic alone, and conjugated ZnO+antibiotic NPs were studied against six microorganisms. Finally, the conjugates with specific antibiotics used in diverse biomedicinal and biotechnological applications were also analyzed.

2 Materials and Methods

2.1 Chemicals and Microorganisms

The following chemicals were procured from Merck (India): zinc nitrate hexahydrate (>98%, AR grade), soluble starch (AR grade), sodium hydroxide (pellet, >98%, AR grade), dimethyl sulfoxide (AR grade), 3-ethyldimethylaminopropyl carbodiimide, N-hydroxysuccinimide, and 3-aminopropyltriethoxysilane (3-APTES). Absolute ethanol (≥99%, AR grade) was purchased from a local vendor. All chemicals were used as received without any pretreatment with high purity. Glass wares viz. test tubes, beakers, Petri plates, conical flasks, and measuring cylinders utilized in the present study were procured from Borosil (India). Double distilled water was used to make the solutions and to rinse all glassware before the experiment.

2.1.1 Antibiotics

The discs containing antibiotics *viz.* ciprofloxacin, ampicillin, and gentamicin were procured from HiMedia (India) for antimicrobial activity against six bacterial strains. Ciprofloxacin, ampicillin, and gentamicin antibiotics were also purchased from HiMedia (India).

2.1.2 Collection of Microorganisms

The following bacterial strains viz. *Pseudomonas aeruginosa* (MTCC-10462), *Bacillus subtilis* (MTCC-441), *Salmonella typhimurium* (MTCC-0968), *Streptococcus* spp. (MTCC-01927), *Klebsiella* spp. (MTCC-07407), and *E. coli* (MTCC-1687) were collected from Microbial Type Culture Collection (MTCC), Chandigarh. All strains were grown at room temperature on the borosilicate glass culture petri plates after providing suitable nutrients and growth conditions. Three antibiotic discs comprising ciprofloxacin, ampicillin, and gentamicin were employed against six bacterial strains to evaluate antimicrobial activity.

2.1.3 Sub-culturing of Microorganisms

Continuous sub-refined or culturing was used to maintain the pure culture of microorganisms on a nutrient agar slant medium. These cultures were kept at 4 °C for further research.

2.2 Functionalization of ZnO NPs

2.2.1 Synthesis of ZnO NPs

ZnO NPs were synthesized using the top-down approach, which is widely used in laboratorial studies; 0.5 gm of soluble starch was dissolved in 50 ml (1% soluble starch) of lukewarm double−distilled water in a round bottom flask under vigorous stirring. Zinc nitrate hexahydrate, 14.87 g, was added slowly under constant stirring. The mixture was further stirred for 60 min to obtain a homogeneous solution at 85 °C. After complete dissolution, 300 ml of 0.2 M sodium

hydroxide was added dropwise while stirring continuously. The reaction solution was incubated overnight after 2 h of stirring. The supernatant solution was discarded carefully, and the remaining solution was centrifuged at 10,000 rpm for 10 min. The obtained nanoparticles were rinsed twice with double−distilled water to eliminate extra starch. The obtained solid was dried at 80 °C overnight. The resultant solid particles were designated as ZnO NPs. Figure 1 shows the detailed synthesis of ZnO NPs.

2.2.2 Amine-functionalization of ZnO NPs

ZnO NPs were functionalized with an amine group using (3−aminopropyl) triethoxysilane (APTES) via co−condensation reaction [13, 14]. In brief, 20 mg of ZnO NPs were dispersed in 20 ml of DMSO under continuous sonication (20 kHz, power = 100W) with an ultrasonic bath for 60 min. The resulting solution was poured into a round bottom flask. The reaction was carried out by adding 500 µL of 3−APTES in the round bottom flask containing sonicated solution and refluxed at 120 °C for 120 min. The amine−functionalized ZnO NPs were centrifuged at 5000 rpm and washed several times with absolute ethanol to ensure complete removal of unreacted 3-APTES. These nanoparticles were dried under a vacuum at 60 °C overnight.

2.2.3 Conjugation of Antibiotics with ZnO NPs

Three different antibiotics viz. ciprofloxacin, ampicillin, and gentamicin were chemically conjugated with amine-functionalized ZnO NPs using N-(3-dimethylaminopropyl)-N'-ethylcarbodiimide (EDC) and N-hydroxysuccinimide (NHS). Briefly, 10 mg of ciprofloxacin was dissolved in a 20-ml solution of DMSO (1:1 ratio) under sonication (20 kHz, power = 100 W) to make the solution homogeneous. EDC (5 mg) and NHS (5 mg) were added slowly to the prepared solution and sonicated for 15 min. The pH of the mixture was set to 6 and stirred for 120 min in a dark chamber. After activation of ciprofloxacin, 20 mg of amine-functionalized ZnO NPs were combined in 20 ml of DMSO (1:1 ratio) and dropped into the antibiotic-containing solution dropwise under sonication. The solution was left to agitate overnight before being centrifuged. The antibiotic-conjugated ZnO NPs were centrifuged at 5000 rpm and washed several times with absolute ethanol to ensure the complete removal of unreacted chemicals. These nanoparticles were dried under a vacuum at 60 °C overnight. A similar methodology was adopted for ampicillin and gentamicin to prepare the conjugate with amine-functionalized ZnO NPs. Figure 1 describes the detailed steps for the functionalization of ZnO NPs.

To investigate the antibacterial activities of antibiotics alone, separate experiments were performed using discs

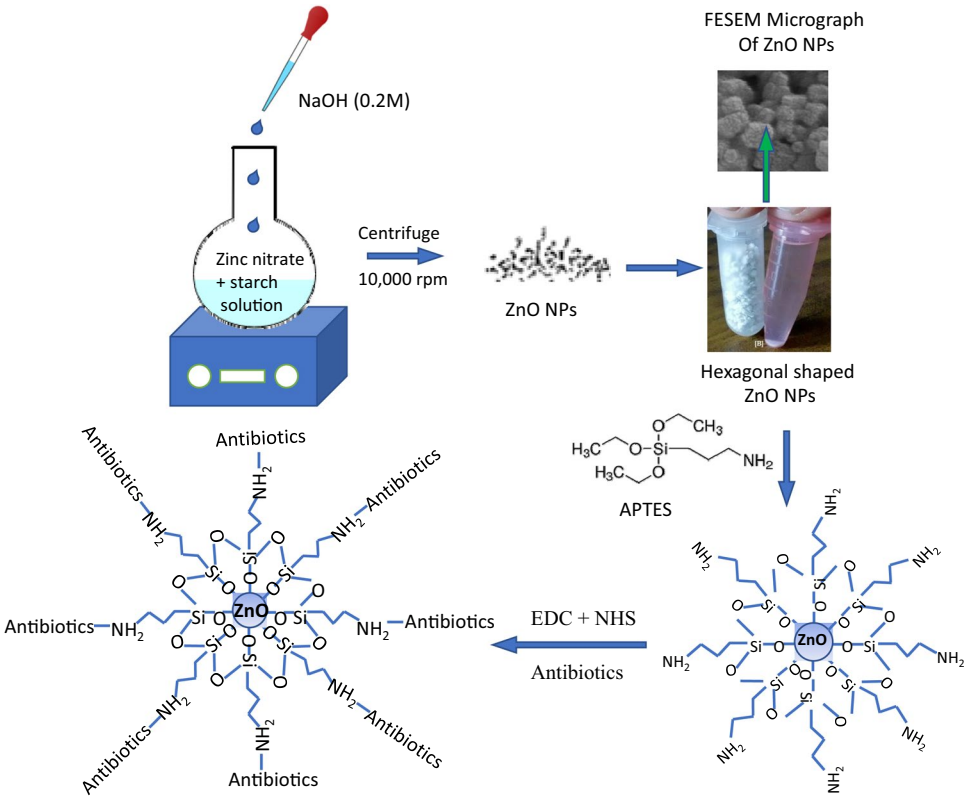

Fig. 1 Schematic representation of the synthesis of ZnO NPs, surface modification of ZnO NPs with APTES, and conjugation of antibiotics on ZnO NPs

containing antibiotics viz. ciprofloxacin, ampicillin, and gentamicin.

2.3 Characterization of Nanoparticles

XRD analysis of nanoparticles was carried out using an X-ray diffractometer (Bruker D8 Discover) equipped with a nickel filter and Cu–Kα radiation at room temperature. XRD scan of the nanoparticles was recorded from 20 to 80°. The crystallite sizes of nanoparticles were determined by using Scherrer's equation. Ultraviolet–visible (UV–Vis) spectra of the samples were carried out using a UV-Vis spectrophotometer V-530 (JASCO). The surface morphology of nanoparticles was analyzed with transmission electron microscopy (Talos F200i) and scanning electron microscopy (Prisma E 210).

2.4 Antimicrobial Activities

A standard disc diffusion method for antimicrobial susceptibility was carried out to assess the zones of inhibition. The broth/agar medium was made using 1 g of beef extract, 1 g of peptone, and 0.5 g of sodium chloride diluted in 100 ml of double distilled water. The media were sterilized before being deposited into Petri dishes for 30 min. After the solidification of nutrient agar, 100 µl of inoculum of different microorganisms was spread on nutrient agar plates to grow culture overnight [2]. A uniform diameter of small holes was prepared on the Petri plate to create a similar space for inhibition. Therefore, a 5-mm diameter of 3−4 holes was made across the Whatman filter paper in equidistant. Steriled Whatman filter paper was placed, and the agar sample was removed through a syringe to prepare the same size of holes on the ##Petri plate; 50 mg/L of zinc oxide NPs with different initial concentrations and antibiotics containing discs was plunged inside the holes of Petri plate. The Petri plates containing the test microorganisms and antibiotic discs/ZnO NPs were allowed to grow at 37 °C for 24−48 h. The plates were analyzed to identify the inhibition zones around the disc. The distance across the inhibition zone was determined with a measuring scale, and the mean size of the inhibition zone for every organism was recorded in centimeter length.

2.5 Colony Forming Unit (CFU) Assay

Bacteria *E. coli* was assayed for CFU measurements on the nutrient agar medium containing 5% of peptone and 1.5% agar. Different starting concentrations of ZnO NPs were used on the samples, ranging from 0.1 to 0.8M. The samples were diluted to 10^9 folds to obtain isolated colonies of microorganisms and incubated at 37 °C for 24 h. The numbers of CFU were counted as

$$\text{CFU/ml} = \text{Colonies/Amount plated (ml)} \times \text{Dilution factor}$$

2.6 Toxicity Estimation of ZnO NPs

ToxTrak™ test was employed to assess the toxicity of chemically produced ZnO NPs, and the percentage inhibition for gram-negative (*E. coli*) and gram-positive (*B. subtilis*) bacterial strains was calculated [15, 16]. Four broth test tubes with 25 g/ml *E. coli* and *B. subtilis* cultures were split into two groups: K_1 for *B. subtilis* and K_2 for *E. coli*. The first to second test tubes are labeled K_1, and the third to fourth tubes are labeled K_2. To determine the toxicity of ZnO NPs against *B. subtilis*, the first test tube of the K_1 group was labeled as a control, and the second test tube was labeled as a sample containing 1 ml of ZnO NPs. To determine the toxicity of ZnO NPs against *E. coli*, the third test tube of the K_2 group was labeled as a control, and the fourth test tube of the K_2 group was labeled as a sample with 1 ml of ZnO NPs; 40 µl of resazurin dye was added to each test tubes of both the groups (K_1 and K_2) and incubated for 4 h. After adding resazurin dye, absorption readings were taken at 1-h intervals for 4 h in all samples. Resazurin dye indicates oxidation/reduction in cell viability tests for mammalian and bacterial cells. Among the initial applications of resazurin dye was to measure bacterial content in the milk [11, 12]. The toxicity of ZnO NPs was determined using the resazurin dye. The percentage inhibition is calculated using the following equation:

$$\text{Calculate the\%inhibition} = 1 - \left(\frac{\Delta A_{\text{sample}}}{\Delta A_{\text{control}}}\right) \times 100$$

where ΔA_{sample} is the changes/differences in absorbance for the initial and final sample with ZnO NPs. $\Delta A_{\text{control}}$ is the changes/differences in absorbance for the initial and final sample without ZnO NPs (with culture only)

3 Results and Discussion

3.1 XRD Analysis

The crystal phase and purity of the ZnO NPs were investigated by XRD analysis, as shown in Fig. 2A. The XRD pattern of the ZnO NPs displays sharp diffraction peaks indexed to (1 0 0), (0 0 2), (1 0 1), (1 0 2), (1 1 0), (1 0 3), (2 0 0), (1 1 2), (2 0 1), (0 0 4), and (2 0 2) planes, which are in well accordance with the standard data for ZnO (JCPDS Card No. 36-1451). The wurtzite lattice parameters, e.g., the values of d-spacing between adjacent crystal planes (h k l), were calculated from Bragg's equation, given as $n\lambda = 2d \sin\theta$, where n is the order of diffraction (an integer, $n =$

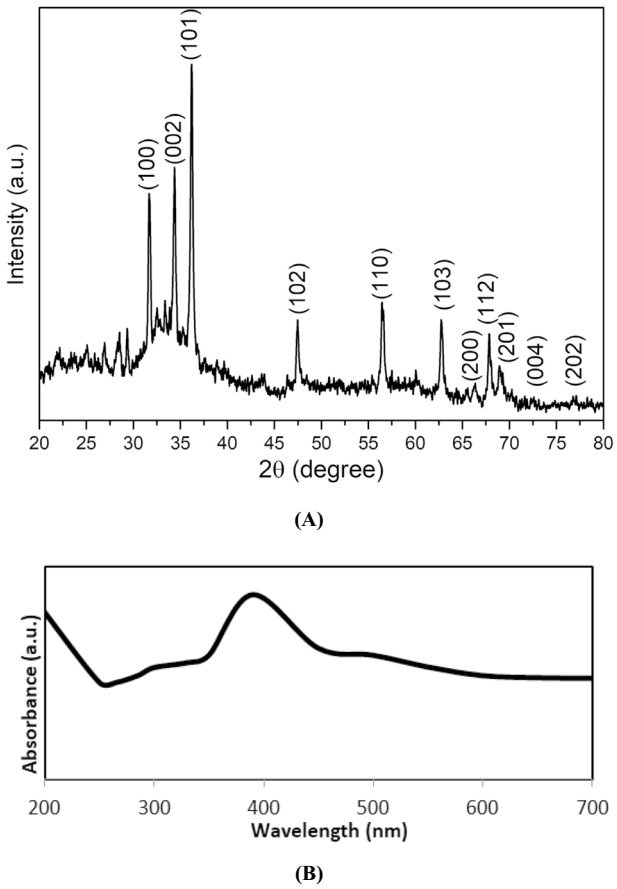

Fig. 2 (**A**) X-ray diffraction (XRD) pattern. (**B**) UV-Vis spectra of ZnO NPs

1), λ is the X-ray wavelength of CuKα (1.5406 Å) radiation wavelength, d is the interplanar spacing, and θ is the Bragg diffraction angle.

The average crystallite size was calculated from the XRD peak width of (1 0 1) based on the Debye–Scherrer equation [17].

$$D = \frac{K\lambda}{\beta_{hkl}\,\mathrm{Cos}\theta}$$

where K is the shape factor (~0.89), λ is the wavelength of Cu−Kα (1.54059 Å) radiation, D is the crystallite size, θ is the Bragg diffraction angle, β is the full width at half maximum (FWHM) of the selected diffraction peak corresponding to the 1 0 1 plane the peak located at $2\theta = 36.25^{O}$, and θ is the Bragg's angle of diffraction (Table 1). The crystalline size of ZnO NPs obtained is 24.84 nm. The XRD pattern shows that ZnO forms a pure phase without any impurities. Kumar et al. (2013) [17] synthesized ZnO NPs and studied the calcination effect on the crystal size using X-ray diffraction analysis. Calcination temperature enhances the intensity of the peaks, resulting in increased crystallinity.

Table 1 X-ray diffraction pattern of ZnO NPs

Peak 2 θ	Θ	smQ/θ	d = n λ/2 sin θ (Å)	d/nm	Plane
31.75	15.87	0.261	2.951	0.2951	100
34.44	17.22	0.294	2.620	0.2620	002
36.25	18.12	0.310	2.484	0.2484	101
67.91	33.95	0.552	1.395	0.1395	112
76.95	38.47	0.591	1.303	0.1303	202

3.2 UV–vis Analysis

The conversion of zinc nitrate hexahydrate to ZnO NPs was confirmed by the UV–vis spectra. The color change in the reaction mixture solution was observed through visual observation in the aqueous solution. Figure 2B shows the absorption spectroscopy of ZnO NPs in the range of 200 to 700 nm at room temperature. The spectrum of ZnO NPs shows a maximum absorption peak at 390 nm ($\lambda_{max} < 400$ nm), which can be consigned to the intrinsic band gap absorption of ZnO NPs due to the transition of electrons from the valence band to the conduction band ($O_{2P} \rightarrow Zn_{3d}$) [18].

3.3 Scanning Electron Microscopy Analysis

Scanning electron microscopy (SEM) images help in the interpretation of the surface morphology of ZnO NPs. The uniform hexagonal-shaped ZnO NPs were produced during synthesis, as shown in Fig. 3A. The average size of ZnO nanoparticles was observed at 200 nm depicted. However, the micrograph also shows the agglomeration between the nanoparticles. A similar observation was depicted by Arora et al. (2014) [19] in the synthesis of ZnO NPs.

3.4 Transmission Electron Microscopy Analysis

Transmission electron microscopy (TEM) images provide additional information about the morphology, shape, distribution profile, and particle size. The hexagonal-shaped ZnO NPs were observed through TEM analysis. It may be possible that ZnO nanoparticles could immediately agglomerate during synthesis due to the Vander wall forces of attraction in the presence of water. In addition, the high polarity of the water causes individual ZnO sub-crystals to grow up separately and finally assemble to form secondary ZnO NPs; all this is possible due to the capping ability of starch. The TEM analysis also suggested the agglomeration of ZnO nanoparticles, as shown in Fig. 3B. An average particle size of 26 nm was determined by TEM analysis and agreed well with SEM analysis. High-resolution transmission electron microscope (HR-TEM) confirms the high crystallinity of ZnO NPs, as shown in Fig. 3C. The

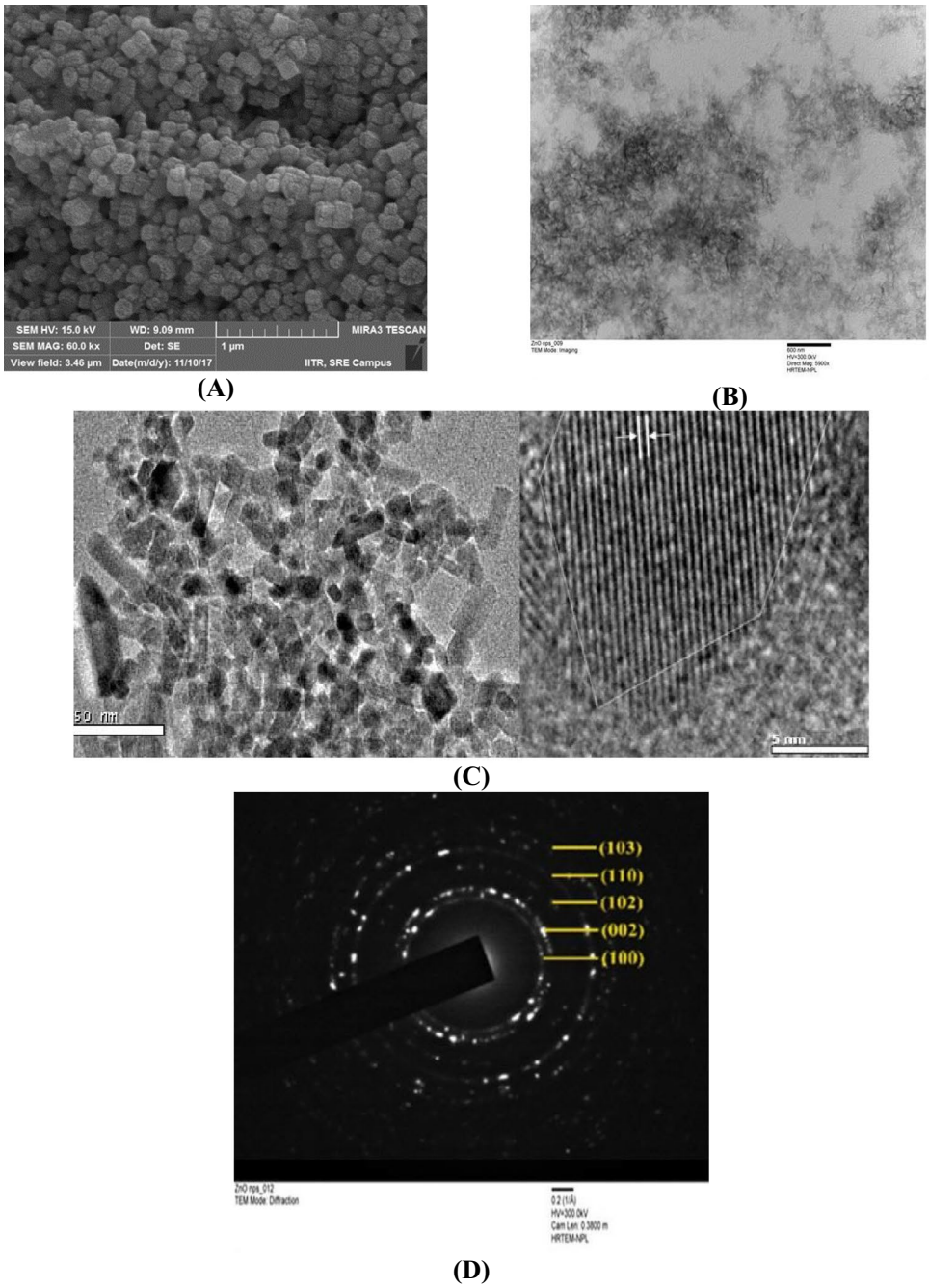

Fig. 3 (**A**) SEM image. (**B**) TEM image. (**C**) HR−TEM image with high magnifications. (**D**) SAED pattern of ZnO NPs

selected area electron diffraction (SAED) pattern of ZnO NPs clearly indicates the crystalline (bright spots) or polynanocrystalline (as shown in Fig. 3D). The SAED pattern depicts diffraction rings of the synthesized ZnO NPs at (1 0 0), (0 0 2), (1 0 2), (1 1 0), and (1 0 3) lattice planes, which indicates that the particles are well crystallized [7, 20, 21].

3.5 Antimicrobial Activity of ZnO NPs Against Pathogens

Antibacterial assays are carried out using the disc diffusion method. Here, bacterial isolates were on nutrient agar media at 37 °C temperature for 24 h. The zone of inhibition was studied after 24 h of incubation. Various doses of ZnO NPs

were tested on six bacteria (*Klebsiella species, Salmonella typhimurium, Pseudomonas aeruginosa, Escherichia coli, Bacillus subtilis*, and *Streptococcus species*). The ZnO NPs were diluted as 100%, 70%, 50%, and 20% by the addition of double distilled water. A 100% concentration of ZnO NPs was shown to be highly effective against all microbiological species. It was observed that the zone of inhibition was maximum (3.4 cm) in *Klebsiella* and minimum (0.4 cm) in *E. coli* species in Table 2. Supplementary Fig. S1 shows the zone of inhibition of discs containing the ZnO NPs. Various inhibitory mechanisms for ZnO nanoparticles' antibacterial activity could be explained as follows.

3.5.1 Release of ROS

The antimicrobial activity includes the release of reactive oxygen species (ROS) from the surface of the ZnO NPs. ROS causes oxidative stress by damaging cellular proteins, cell membranes, and DNA. The ZnO NPs are catalyzed by light energy viz. UV and visible light for redox reactions. Its unique electrical configuration, which includes a vacant valence band and an occupied conduction band, explains this. The produced electrons and holes react with other oxygen species viz. H_2O and O_2 are adsorbed on the surface or have the probability of recombination. Generated electrons and hole pairs have the probability of generating reactive oxygen species inside the suspension by following steps [1, 4]:

$$ZnO + hv \rightarrow e^- + h^+$$

$$h^+ + H_2O \rightarrow {}^{\bullet}OH + H^+$$

$$e^- + O_2 \rightarrow O_2^{\bullet -}$$

$$O_2^{\bullet -} + H^+ \rightarrow HO_2^{\bullet}$$

$$HO_2^{\bullet} + H^+ + e^- \rightarrow H_2O_2$$

Hydrogen peroxide has the ability to enter the cell membrane and kill bacteria.

The chemical species generated from the surface of ZnO NPs damage the cell wall, and subsequently, the oxidative damage then spreads to the inner peptidoglycan layer and cytoplasmic membrane. The slow leakage of proteins and RNA and rapid outflow of K^+ ions result as the primary cause of bacterial death. The dissociation of carboxylic groups caused the −ev charge on the bacterial cell wall. ZnO NPs possess a positive charge with a zeta potential of +24 mV at the surface. The electrostatic force between positively charged ZnO and negatively charged bacterial cells wall causes cell wall rupture, and damage occurred by entering into the cell [3, 4, 22].

3.5.2 Release of Zn^{2+}

Another plausible mechanism for the antibacterial activity of ZnO NPs is the release of Zn^{2+} ions from the surface of nanoparticles. It can damage the cell membrane and enter the intracellular contents present in the microbial cell. Wang et al. (2014) [23] studied the effect of ZnO nanoparticles in ZnO/GO composites to achieve superior antibacterial activities with the typical bacterium *Escherichia coli* and HeLa cell. It was observed that 30% of Zn^{2+} ions quickly dissolved from the ZnO/GO composites at the beginning. The close contact increased the local Zn^{2+} ion concentration pitting on the bacterial cell membrane as well as the permeability of the bacterial cell membrane, resulting the bacterial death. Esmailzadeh et al. (2016) [5] investigated the antibacterial growth of low-density polyethylene-containing ZnO NPs on *Bacillus subtilis* and *Enterobacter aerogenes*. They observed that *B. subtilis* as gram-positive bacteria were more sensitive to ZnO NPs containing nanocomposite films compared with *E. aerogenes* as gram-negative bacteria. They also studied the release of metal ions from the surface of ZnO NPs containing nanocomposite. Motshekga et al. (2015) [24] developed chitosan-based nanocomposites with bentonite-supported silver and zinc oxide nanoparticles to achieve complete inactivation of bacteria *viz.* gram-negative *Escherichia coli* and gram-positive *Enterococcus faecalis* in water.

Table 2 Effect of initial concentration of ZnO NPs with bacterial species

Concentration of ZnO NPs	*Bacillus subtilis*	*Klebsiella spp*	*Pseudomonas aeruginosa*	*Salmonella typhimurium*	*E. coli*	*Streptococcus spp*
20%	0.1 ± 0.02	2 ± 0.17	0.7 ± 0.06	0.6 ± 0.01	0.2 ± 0.01	0.8 ± 0.06
50%	0.3 ± 0.03	2.4 ± 0.21	1.3 ± 0.10	0.9 ± 0.05	0.2 ± 0.01	0.9 ± 0.06
70%	0.9 ± 0.07	2.3 ± 0.20	1.5 ± 0.13	1.0 ± 0.04	0.3 ± 0.02	1.3 ± 0.10
100%	1.1 ± 0.11	3.4 ± 0.29	1.7 ± 0.19	1.1 ± 0.05	0.4 ± 0.03	1.5 ± 0.12

All the data values are presented as mean ± SE

Table 3 Effect of different antibiotics with bacterial species

Antibiotics	*Bacillus subtilis*	*Klebsiella spp*	*Pseudomonas aeruginosa*	*Salmonella typhimurium*	*E. coli*	*Streptococcus spp*
Gentamicin	2 ± 0.12	4.3 ± 0.28	2.7 ± 0.14	1.1 ± 0.08	0.6 ± 0.02	1.5 ± 0.12
Ampicillin	2.3 ± 0.14	4.4 ± 0.26	2.8 ± 0.16	0.7 ± 0.04	0.5 ± 0.02	4 ± 0.23
Ciprofloxacin	1.5 ± 0.13	5 ± 0.32	0.1 ± 0.02	1.3 ± 0.10	1.1 ± 0.11	1 ± 0.09

3.5.3 Direct Contact of ZnO NPs with Cell Membrane

On the other hand, interactions of ZnO NPs with the bacterial cell membranes and the damage on the bacterial surface have been suggested as a responsible step for the antibacterial activity. In this respect, Zhang et al. (2007) [25] studied the effects of particle size, concentration, and the use of dispersants on the antibacterial activity of ZnO NPs against *E. Coli*. The antibacterial activity increases with the ZnO NPs loading and reducing the size of NPs. The direct interaction between ZnO NPs and the bacterial cell wall membrane was the primary step for damaging the surfaces.

3.6 Antibacterial Activity of Antibiotics

The three antibiotic discs comprising ciprofloxacin, ampicillin, and gentamicin were employed against six bacterial strains to evaluate antimicrobial activity. Supplementary Fig. S2 shows the inhibition zones for antibiotics. Among all, three antibiotics viz. *Klebsiella spp and Streptococcus spp* exhibited maximum zone of inhibition as 4.4 cm and 4.0 cm, with ampicillin, respectively. For gentamycin and ampicillin, *Klebsiella spp* also resulted in a higher zone of inhibition, as shown in Table 3. Antibiotics inhibit bacterial cell wall synthesis of *Klebsiella spp*. by binding to peptidoglycan-synthesizing enzymes [26]. This could result in the deactivation of cell activity or killing the *Klebsiella spp*. cell. The minimum inhibition zone of 0.1 cm was analyzed by ciprofloxacin against *E. coli*. *E. coli* shows a higher genetic resistance capacity toward the antibiotic for cell wall damage or direct attack. Among all the six bacteria, *Klebsiella spp*. was highly susceptible to all three antibiotics, as given in Table 3. The plausible explanation is that antibiotics block the vital processes of bacteria by disrupting the structures in the bacterial cell. This step either kills the bacterium or slows down bacterial growth in the medium. Depending on this efficacy, the bactericidal activity of antibiotics showed different zones of inhibition with different bacteria. In the case of *Klebsiella spp*., all three antibiotics kill many bacteria and generate a larger circle of inhibition zone.

3.7 Combination of ZnO NPs and Antibiotics

The effect of varying concentrations of ZnO NPs in conjunction with three antibiotics was observed for bacterial species with the disc diffusion method. Supplementary Fig. S3 shows the zone of inhibition for a disc containing antibiotics

Table 4 Effect of initial concentration of ZnO NPs in the presence of different antibiotics with bacterial species

(A)									
Concentration	*Bacillus subtilis*			*Klebsiella spp*			*Pseudomonas aeruginosa*		
	Gentamicin	Ampicillin	Ciprofloxacin	Gentamicin	Ampicillin	Ciprofloxacin	Gentamicin	Ampicillin	Ciprofloxacin
20c	0.5 ± 0.04	0.4 ± 0.02	0.3 ± 0.01	1.1 ± 0.10	0.8 ± 0.04	1.5 ± 0.16	0.3 ± 0.01	0.4 ± 0.02	0.8 ± 0.04
50c	1.2 ± 0.09	1.1 ± 0.10	2 ± 0.14	1.9 ± 0.13	2.0 ± 0.14	3.9 ± 0.30	2.2 ± 0.16	0.7 ± 0.036	2.5 ± 0.17
70c	2.2 ± 0.16	1.7 ± 0.17	2.6 ± 0.19	4.1 ± 0.31	3 ± 0.22	4.7 ± 0.36	2.8 ± 0.20	1.5 ± 0.16	3 ± 0.21
100c	2.6 ± 0.17	2.4 ± 0.16	2.9 ± 0.21	4.6 ± 0.35	4.4 ± 0.33	5.2 ± 0.37	3.2 ± 0.24	2.9 ± 0.21	3.4 ± 0.25
(B)									
Concentration	*Salmonella typhimurium*			*E. coli*			*Streptococcus spp*		
	Gentamicin	Ampicillin	Ciprofloxacin	Gentamicin	Ampicillin	Ciprofloxacin	Gentamicin	Ampicillin	Ciprofloxacin
20c	0.9 ± 0.05	0.4 ± 0.02	0.5 ± 0.02	0.3 ± 0.01	0.4 ± 0.02	0.7 ± 0.06	0.6 ± 0.03	1 ± 0.09	0.8 ± 0.04
50c	2 ± 0.14	0.9 ± 0.05	1.8 ± 0.13	0.8 ± 0.04	0.9 ± 0.05	1.6 ± 0.16	1.4 ± 0.12	1.7 ± 0.17	1.5 ± 0.13
70c	2.9 ± 0.21	1.5 ± 0.13	2.5 ± 0.18	1.5 ± 0.13	1.2 ± 0.12	2.6 ± 0.19	2 ± 0.14	3.2 ± 0.24	2 ± 0.14
100c	3.5 ± 0.26	2 ± 0.14	3 ± 0.22	2.5 ± 0.18	2 ± 0.14	3.2 ± 0.24	3 ± 0.22	3.8 ± 0.27	2.8 ± 0.21

Table 5 Synergetic study on antibacterial activities with bacterial species

(A)

	Bacillus subtilis			*Klebsiella spp*			*Pseudomonas aeruginosa*		
	Gentamicin	Ampicillin	Ciprofloxacin	Gentamicin	Ampicillin	Ciprofloxacin	Gentamicin	Ampicillin	Ciprofloxacin
ZnONP 100c	1.1	1.1	1.1	3.4	3.4	3.4	1.7	1.7	1.7
Antibiotic	2	2.3	1.5	4.0	4.0	4.9	2.7	2.8	0.1
Antibiotic + ZnO NP (100c)	2.6	2.4	2.9	4.6	4.4	5.2	3.2	2.9	3.4

(B)

	Salmonella typhimurium			*E. coli*			*Streptococcus spp*		
	Gentamicin	Ampicillin	Ciprofloxacin	Gentamicin	Ampicillin	Ciprofloxacin	Gentamicin	Ampicillin	Ciprofloxacin
ZnO NP (100c)	1.1	1.1	1.1	0.4	0.4	0.4	1.5	1.5	1.5
Antibiotic	1.1	0.7	1.3	0.6	0.5	1.1	1.5	4	1
Antibiotic + ZnO NP (100c)	3.5	2	3	2.5	2	3.2	3	3.8	2.8

and ZnO NPs. Here, the combination of the highest concentration of ZnO NPs with antibiotics showed the highest zone of inhibition than ZnO alone and antibiotics alone. *Klebsiella* species showed the highest percentage inhibition zone and *Pseudomonas species* with a combination of ciprofloxacin + ZnO NPs, followed by ZnO NPs + gentamicin combination for both. All of these combinations showed a higher zone of inhibition as compared to antibiotic and ZnO NPs alone.

It is evident from Table 4 that the antimicrobial activity of each combination has been improved. For *Klebsiella spp*, the combination of ZnO + antibiotics shows a higher inhibition zone of 4.6 cm, 4.4 cm, and 5.2 cm for gentamycin, ampicillin, and ciprofloxacin, respectively. Fadwa et al. (2021) [6] isolated *E. coli* and *A. baumannii* bacterial species from various clinical samples to determine the MIC and FICI of meropenem, colistin, ciprofloxacin, and a combination of meropenem, colistin, and ciprofloxacin with ZnO NPs. Abo-Shama et al. (2020) [27] investigated antibacterial activity for Ag NPs and ZnO NPs. Both NPs had enhanced the antibacterial activity with increased concentration against gram-negative bacteria (*E. coli* and *Salmonella* spp) and gram-positive bacterium (*Staph. aureus*) and no effect on *C. albicans*. Antibiotics (azithromycin, oxacillin, cefotaxime, cefuroxime, fosfomycin, and oxytetracycline) had a considerably greater synergistic impact against *E. coli* in the presence of ZnO NPs compared to antibiotics alone. All of these observations supported the current findings of ZnO NPs, which demonstrate antibacterial activity, but the synergistic effect against bacteria was significantly greater.

Ciprofloxacin shows the highest bacteriocidal activity against klebsiella species (among six bacterial pathogens and less susceptible in Pseudomonas). Ciprofloxacin is a fluoroquinolone antibiotic with a broad spectrum of antibacterial action [28]. Masadeh et al. (2015) [29] investigated that the antibiotic interacts with bacterial topoisomerases resulting in the generation of oxidative radicals toward bacterial death. Ciprofloxacin antibiotic + ZnONPs + conjugates could be more efficient for bacteriocidal activity. In the case of gentamycin, it shows the highest bactericidal activity against *Klebsiella* species and is less susceptible to *E. Coli*. It is an aminoglycoside antibiotic that works by interfering with bacterial protein synthesis to inhibit bacterial growth. Mader (2005) [30] found that gentamycin binds with 30S and 50S ribosomal subunits. It damages the bacterial cell wall membrane resulting in concentration-dependent bacterial killing. Its mechanism of action inhibits bacterial protein synthesis by binding to 30S and 50S ribosomes. However, ampicillin inhibits bacterial cell wall synthesis by binding to peptidoglycan-synthesizing enzymes [26, 28]. Kohanski et al. (2010) [28] reported that ampicillin blocks the cross-linking of peptidoglycan units. The cell wall synthesis inhibitor can change cell size and shape, induce cellular stress responses, and culminate in cell lysis. Table 5 shows the

Table 6 Effect of initial concentration of ZnO NPs on *E. coli*

Dilution	CFU/ml	ZnO NPs (µg/ml)
$_{10}-6$	3.2×10^6 CFU/ml	100
$_{10}-7$	3.9×10^7 CFU/ml	90
$_{10}-8$	4.1×10^8 CFU/ml	80
$_{10}-9$	4.6×10^9 CFU/ml	70

Table 7 Toxicity analysis of control and different broths treated with ZnO NPs

Incubation period with dye (h)	*B. subtilis*		*E coli*	
	Control (ΔAc)[#]	ZnO NPs (ΔAS)[#]	Control (ΔAc)[#]	ZnO NPs (ΔAS)[#]
0	2.685	2.125	2.885	3.256
1	2.356	1.563	2.356	2.895
2	2.231	1.325	1.568	2.562
3	1.456	1.123	1.256	2.321
4	0.856	0.756	0.958	1.986

[#]Absorption value of control and different broths treated with ZnO NPs

synergetic antibacterial behavior of the combined process of ZnO + antibiotic with ZnO alone and antibiotic alone.

3.8 Analysis of CFU Measurement with *E. coli*

E. coli was selected for CFU measurement to identify colony formation in the presence of ZnO NPs in dilutions. For the quantitative determination of the antibacterial activity of ZnO NPs, the bacterial sample was serially diluted in a range of concentrations from 10^{-6} to 10^{-9}. Then, 100 µl of bacterial suspension (approximately 105 CFU/ml are found in 100 µl cell suspensions) was speared on agar plates. After that, all petri discs were incubated at 37 °C for 24 h. *E. coli* colonies were manually counted after the incubation. The CFU of ZnO NPs against *E. coli* species is presented in Supplementary Fig. S4 and Table 6. The number of CFU/ml has increased dramatically with the decreasing concentration of ZnO NPs. Paul and Ban (2014) [31] investigated the antimicrobial behavior of *E. coli* in the face of ZnO NPs. They discovered that when the concentration of ZnO NPs increased, the number of CFU decreased dramatically.

3.9 Toxicity Analysis

Table 7 shows the toxicity analysis of *Bacillus subtilis* and *E. coli* for control and ZnO-loaded systems. These concentrations of treated samples with ZnO NPs (AS) were determined at 603 nm using a UV spectrophotometer. To determine percentage inhibition, first, the differences in absorbance for the control (ΔAc) and ZnO NPs were calculated. The percentage inhibition is represented by the following equation: Percentage inhibition (PI) = [1−(ΔAs/ΔAc)]×100.

3.9.1 Sample calculation

For control: $\Delta Ac = -1.529\ (K_1)$ and $-1.414\ (K_2)$

For ZnO NPs: $\Delta A_S = -0.369\ (K_1)$ and $-0.470(K_2)$

3.9.2 Toxicity of ZnO NPs sample

Toxicity of ZnO NPs in the K_1 group by entering the absorption values:

$$PI = \left[1 - (-0.369/-1.529)\right] \times 100 = \mathbf{75.86}\ \%$$

Toxicity of ZnO NPs in the K_2 group by entering the absorption values:

$$PI = \left[1 - (-0.4700/-1.414)\right] \times 100 = \mathbf{66.76}\ \%$$

Toxicity of ZnO NPs data clearly shows that the toxic impact values and percentage inhibition of ZnO NPs are slightly higher, 75.86% for K_1 (*B. subtilis*) than 66.76% for K_2 (*E. coli*). The fact that the percentage inhibition of ZnO NPs differed only slightly across the K_1 and K_2 groups implies that the toxic effects of ZnO NPs are the same for all bacterial species. Tyagi et al. (2013) [32] synthesized silver nanoparticles with biological and chemical routes and performed toxicity test on silver nanoparticles using the Tox-Trak™ method; 85.45% and 51.39% of PI on the microflora of the human gut (*B. subtilis*) were obtained with chemical and biological synthesized nanoparticles.

4 Conclusions

ZnO NPs were synthesized using a top-down approach which is widely used in laboratories. Synthesized ZnO NPs were functionalized with amine group using (3-aminopropyl) triethoxysilane via co-condensation reaction to conjugate with antibiotics viz. ciprofloxacin, ampicillin, and gentamicin using N-(3-dimethylaminopropyl)-N'-ethylcarbodiimide and N-hydroxysuccinimide. Bare and functionalized ZnO NPs were characterized with UV–visible spectroscopy, XRD, TEM, and SEM. Bare ZnO NPs, antibiotics, and a combination of ZnO NPs + antibiotics are used against six bacterial strains to evaluate antimicrobial activity. *Klebsiella spp*. was highly susceptible toward bare ZnO NPs, antibiotics, and a combination of ZnO NPs + antibiotics. The mechanisms of the antimicrobial behavior of functionalized ZnO NPs were

discussed. *E. coli* was selected for CFU measurement to identify colony formation in the presence of different dilutions of ZnO NPs. ToxTrak™ test was used to assess the toxicity of chemically synthesized ZnO NPs; 75.86% and 66.76% of inhibition were obtained for gram-positive (*B. subtilis*) and gram-negative (*E. coli*) bacterial strains, respectively.

Supplementary Information The online version contains supplementary material available at https://doi.org/10.1007/s12668-023-01156-4.

Author Contributions **DVSP:** methodology, formal analysis, writing – original draft

KR: conceptualization, investigation, formal analysis, writing – original draft

SS: conceptualization, supervision, writing – review and editing

Funding This research received no specific grant from any funding agency in the public, commercial, or not-for-profit sectors.

Data Availability All materials and data which were generated or analyzed during this study were included in this article.

Code Availability Not applicable.

Declarations

Ethics Approval Not applicable

Consent to Participate Not applicable

Consent for Publication All the authors have read and approved the manuscript and accorded consent for publication.

Competing Interests The authors declare no competing interests.

References

1. Padmavathy, N., & Vijayaraghavan, R. (2008). Enhanced bioactivity of ZnO nanoparticles – An antimicrobial study. *Science and Technology of Advanced Materials, 9*(3) 035004.
2. Stoimenov, P. K., Klinger, R. L., Marchin, G. L., & Klabunde, K. J. (2002). Metal oxide nanoparticles as bactericidal agents. *Langmuir, 18*(17), 6679–6686.
3. Espitia, P. J. P., Soares, N. d. F. F., Coimbra, J. S. D. O. S. R., de Andrade, N. J., Cruz, R. S., & Medeiros, E. A. A. (2012). Zinc oxide nanoparticles: Synthesis, antimicrobial activity and food packaging applications. *Food and Bioprocess Technology, 5*(5), 1447–1464.
4. Dimapilis, E. A. S., Hsu, C. S., Mendoza, R. M. O., & Lu, M. C. (2018). Zinc oxide nanoparticles for water disinfection. *Sustainable Environment Research, 28*(2), 47–56.
5. Esmailzadeh, H., Sangpour, P., Shahraz, F., Hejazi, J., & Khaksar, R. (2016). Effect of nanocomposite packaging containing ZnO on growth of Bacillus subtilis and Enterobacter aerogenes. *Materials Science and Engineering C, 58*, 1058–1063.
6. Fadwa, A. O., Albarag, A. M., Alkoblan, D. K., & Mateen, A. (2021). Determination of synergistic effects of antibiotics and Zno NPs against isolated E. Coli and A. Baumannii bacterial strains from clinical samples. *Saudi Journal of Biological Sciences, 28*(9), 5332–5337.
7. Fowsiya, J., Asharani, I. V, Mohapatra, S., Eshapula, A., Mohi, P., Thakar, N., … Madhumitha, G. (2019). *Self-dual Leonard pairs stabilized synthesis and characterization of ZnO nanoparticles and their role against, 488–495*.
8. Happy, A., Menon, S., Venkat Kumar, S., & Rajeshkumar, S. (2018). Mechanistic study on antibacterial action of zinc oxide nanoparticles synthesized using green route. *Chemico-Biological Interactions*, *286*, 60–70.
9. Hameed, A. S. H., Karthikeyan, C., Sasikumar, S., Senthil Kumar, V., Kumaresan, S., & Ravi, G. (2013). Impact of alkaline metal ions Mg2+, Ca2+, Sr 2+ and Ba2+ on the structural, optical, thermal and antibacterial properties of ZnO nanoparticles prepared by the co-precipitation method. *Journal of Materials Chemistry B, 1*(43), 5950–5962.
10. Yamamoto, O. (2001). Influence of particle size on the antibacterial activity of zinc oxide. *International Journal of Inorganic Materials, 3*(August), 643–646.
11. Anoopkumar-Dukie, S., Carey, J. B., Conere, T., O'Sullivan, E., Van Pelt, F. N., & Allshire, A. (2005). Resazurin assay of radiation response in cultured cells. *British Journal of Radiology, 78*(934), 945–947.
12. Silanikove, N., & Shapiro, F. (2012). In R. P. Victor (Ed.), *Combined assays for lactose and galactose by enzymatic reactions. In Dietary Sugars: Chemistry, Analysis, Function and Effects, Food and Nutritional Components in Focus*. The Royal Society of Chemistry.
13. Guo, Y., Wang, H., He, C., Qiu, L., & Cao, X. (2009). Uniform carbon-coated ZnO nanorods: Microwave-assisted preparation, cytotoxicity, and photocatalytic activity. *Langmuir, 25*(8), 4678–4684.
14. Patra, P., Mitra, S., Debnath, N., Pramanik, P., & Goswami, A. (2014). Ciprofloxacin conjugated zinc oxide nanoparticle: A camouflage towards multidrug resistant bacteria. *Bulletin of Materials Science, 37*(2), 199–206.
15. Liwarska-Bizukojc, E., Olejnik, D., Delbeke, E. I. P., Van Geem, K. M., & Stevens, C. V. (2018). Evaluation of biological properties and fate in the environment of a new class of biosurfactants. *Chemosphere, 200*, 561–568.
16. Toxicity ToxTrak Method 10017 HACH LANGE Manual. (2014). *ToxTrak™ Method* (pp. 1–8). ToxTrak.
17. Kumar, S. S., Venkateswarlu, P., Rao, V. R., & Rao, G. N. (2013). Synthesis, characterization and optical properties of zinc oxide nanoparticles. *International Nano Letters, 3*, 1–6.
18. Zak, A. K., Abrishami, M. E., Majid, W. H. A., Yousefi, R., & Hosseini, S. M. (2011). Effects of annealing temperature on some structural and optical properties of ZnO nanoparticles prepared by a modified sol-gel combustion method. *Ceramics International, 37*(1), 393–398.
19. Arora, A. K., Devi, S., Jaswal, V. S., Singh, J., Kinger, M., & Gupta, V. D. (2014). Synthesis and characterization of ZnO nanoparticles. *Oriental Journal of Chemistry, 30*(4), 1671–1679.
20. Safawo, T., Sandeep, B. V., Pola, S., & Tadesse, A. (2018). Synthesis and characterization of zinc oxide nanoparticles using tuber extract of anchote (Coccinia abyssinica (Lam.) Cong.) for antimicrobial and antioxidant activity assessment. *OpenNano*, *3*(August), 56–63.
21. Khoshhesab, Z. M., Sarfaraz, M., & Asadabad, M. A. (2011). Preparation of ZnO nanostructures by chemical precipitation method. *Synthesis and Reactivity in Inorganic, Metal-Organic and Nano-Metal Chemistry, 41*(7), 814–819.
22. Abebe, B., Zereffa, E. A., Tadesse, A., & Murthy, H. C. A. (2020). A Review on enhancing the antibacterial activity of ZnO: Mechanisms and microscopic investigation. *Nanoscale Research Letters, 15*(1), 190.
23. Wang, Y. W., Cao, A., Jiang, Y., Zhang, X., Liu, J. H., Liu, Y., & Wang, H. (2014). Superior antibacterial activity of zinc oxide/graphene oxide composites originating from high zinc concentration localized around bacteria. *ACS Applied Materials and Interfaces, 6*(4), 2791–2798.

24. Motshekga, S. C., Sinha, S., Onyango, M. S., & Momba, M. N. B. (2015). Applied Clay Science Preparation and antibacterial activity of chitosan-based nanocomposites containing bentonite-supported silver and zinc oxide nanoparticles for water disinfection. *Applied Clay Science, 114*, 330–339.
25. Zhang, L., Jiang, Y., Ding, Y., Povey, M., & York, D. (2007). Investigation into the antibacterial behaviour of suspensions of ZnO nanoparticles (ZnO nanofluids). *Journal of Nanoparticle Research, 9*(3), 479–489.
26. Bangen, K., Hong, N., Louie, A., Mei, G., & Artha, J. T. (2004). The effects of incubation with ampicillin and tetracycline on the expression of the bla and tetA genes of pBR322. *Journal of Experimental Microbiology and Immunology, 5*(April), 23–28.
27. Abo-Shama, U. H., El-Gendy, H., Mousa, W. S., Hamouda, R. A., Yousuf, W. E., Hetta, H. F., & Abdeen, E. E. (2020). Synergistic and antagonistic effects of metal nanoparticles in combination with antibiotics against some reference strains of pathogenic microorganisms. *Infection and Drug Resistance, 13*, 351–362.
28. Kohanski, M. A., Dwyer, D. J., & Collins, J. J. (2010). How antibiotics kill bacteria: From targets to networks. *Nature Reviews Microbiology, 8*(6), 423–435.
29. Masadeh, M. M., Alzoubi, K. H., Khabour, O. F., & Al-Azzam, S. I. (2015). Ciprofloxacin-induced antibacterial activity is attenuated by phosphodiesterase inhibitors. *Current Therapeutic Research - Clinical and Experimental, 77*, 14–17.
30. Mader, D. R. (1996). *Reptile medicine and surgery*. W.B. Saunders Company, Philadelphia, PA, USA.
31. Paul, S., & Ban, D. K. (2014). Synthesis, characterization and the application of ZnO nanoparticles in biotechnology. *International Journal of Advance in Chemical Engineering, and Biological Sciences, 1*(1), 1–5.
32. Tyagi, P. K., Tyagi, S., Verma, C., & Rajpal, A. (2013). Estimation of toxic effects of chemically and biologically synthesized silver nanoparticles on human gut microflora containing Bacillus subtilis. *Journal of Toxicology and Environmental Health Sciences, 5*(9), 172–177.